Electronic Supplementary Information (ESI)

Constructing Cu^0/Cu^+ interfaces on copper foil to boost electrochemical CO_2 reduction to ethylene

Shuiping Zhong,[abc] Bisheng Chen,[a] Ding Tang,[c] Qiuyue Yang,[d] Wei Weng,[*ab] and Xue Feng Lu[*d]

[a] Zijin School of Geology and Mining, Fuzhou University, Fuzhou 350108, China

[b] Fujian Key Laboratory of Green Extraction and High-value Utilization of New Energy Metals, Fuzhou University, Fuzhou 350108, China

[c] Zijin Mining Group Co., Ltd, Shanghang, Longyan 364200, China

[d] State Key Laboratory of Chemistry for NBC Hazards Protection, State Key Laboratory of Photocatalysis on Energy and Environment, College of Chemistry, Fuzhou University, Fuzhou 350116, China

Material

Copper chloride ($CuCl_2$, > 98%) and methanol (CH_3OH, > 99.9%) were purchased from Aladdin (Shanghai, China). Phosphoric acid (H_3PO_4, 85-90%) and potassium hydroxide (KOH, 95%) were purchased from Macklin (Shanghai, China). Potassium bicarbonate ($KHCO_3$, > 99.5%), potassium dihydrogen phosphate (KH_2PO_4, > 99.5%), and sulfuric acid (H_2SO_4, 95-98%) were purchased from Sinopharm Chemical Reagent Co. Ltd (Beijing, China). Copper foil (thickness = 4.5 μm) was purchased from Jingliang Copper Industry Co., Ltd (Shenzhen, China). Nafion-117 proton exchange membrane (Dupont) and Nafion solution (5 wt%) were purchased from Sinero. Carbon paper was purchased from Gaoss Union Photoelectric Technology Co., Ltd (Tianjin, China). CO_2 (99.999%) and Ar (99.999%) were purchased from Huaxinda Industrial Gas Co., Ltd (Fuzhou, China). The ultrapure water (18.25 MΩ cm) was prepared by a UP Water Purification System (JingCheng Instrument Co., Ltd, Qingdao, China).

Electrode preparation

Synthesis of CuCl-Cu

A copper foil with an effective area of 0.5 × 0.5 cm² (1 × 1 cm² for flow-cell) was first immersed in 10% H_2SO_4 for 1 minute, followed by sequential rinsing with deionized water and ethanol, and vacuum-dried at 60°C, then the copper foil was immersed in a 0.1−0.5 M $CuCl_2$ aqueous solution for 3 minutes, rinsed with ethanol, and vacuum-dried to fabricate the CuCl-Cu electrode.

Synthesis of CuCl/CP

A CuCl-Cu electrode was selected, and CuCl particles on its surface were carefully scraped off. The collected CuCl powder (4 mg) was dispersed in an ink comprising 288 μL ethanol, 72 μL deionized water, and 40 μL Nafion solution (5 wt%). The catalyst ink (25 μL) was drop-casted onto a 0.5 × 0.5 cm² carbon paper substrate for H-cell testing, while a 1 × 1 cm² carbon paper was used for flow-cell.

Characterization

X-ray diffraction (XRD) data were collected on a Malvern Panalytical X'pert[3] instrument. Transmission electron microscopic (TEM) images were collected on a Thermo Fisher Talos F200X instrument. Scanning electron microscopic (SEM) images were collected on a Thermo Fisher Phenom Pure G6 instrument. X-ray photoelectron spectroscopy (XPS) data were collected on a Thermo Fisher ESCALAB QXi instrument, the binding energy data were calibrated with reference to the C 1s signal at 284.8 eV. The electrochemical characteristics data were collected by the CHI 760E electrochemistry workstation.

Electrochemical Measurements

The electrochemical measurements were conducted on a typical H-cell with a three-electrode system, in which the anode and cathode reaction cells were separated by a Nafion-117 proton exchange membrane. The electrolyte was composed of 0.5 M $KHCO_3$ aqueous solution, with Raw Cu foil, CuCl/CP and CuCl-Cu as the working electrode (cathode), Ag/AgCl (saturated with KCl) as the reference electrode, and 1 * 10 * 10 mm platinum sheet as the counter electrode (anode). High-purity CO_2 was passed into the electrolyte to saturation (30 mL/min for 20 min) before the experiment,[1] and CO_2 was continuously supplied to the electrolyte (10 mL/min) during the experiment. LSV testing was conducted at a scanning speed of 5 mV/s. EIS measurements were obtained using an amplitude of 5 mV and frequency range from 0.01 Hz to 10000 Hz with an applied potential of −0.1 V (vs. Ag/AgCl). Potentials while measured vs. Ag/AgCl (saturated with KCl) are converted to the RHE scale using the formula:

$$E\,(\text{vs. RHE}) = E\,(\text{vs. Ag/AgCl}) + 0.197\ \text{V} + 0.0591\ \text{V} \times \text{pH}$$

The flow cell consists of an anion-exchange membrane (Selemion AMN/N type 1, AGC Inc), a stability chamber to protect liquids from entering the gas chromatography (GC), a commercial Ti/IrO_2 anode and a gas diffusion electrode (GDE) sandwiched between the catholyte and gas-flow chamber. The substrate side of the GDE faced the gas-flow chamber and the catalyst side faced the catholyte chamber.[2] The catholyte was 2 M KOH and the anolyte was 0.2 M $KHCO_3$. High-purity CO_2 was continuously supplied to the gas-flow chamber (20 mL/min) during the experiment. All electrochemical experiments were performed at room temperature (20 °C). Upon completion of the electrolysis, a portion of the electrolyte (5 mL) was extracted for its utilization in high-performance liquid chromatography (HPLC) analysis.

Products analysis

GC analysis

The gas products of CO_2 electroreduction were monitored by a SHIMADZU GC-2014C systematic gas chromatography coupled with a thermal conductivity detector (TCD) and a flame ionization detector (FID), using mixed gases of different ratios to draw a standard curve to calculate the Faraday efficiency of the product, running Ar (99.999%) as a carrier gas.

HPLC analysis

The concentration of formate products was detected by SHIMADZU LC-16 high-performance liquid chromatograph. The chromatographic column was C18-AQ (5 μm, 4.6×250 mm, Shim-pack GIST, SHIMADZU). The eluting method was gradient elution, mobile phase A was CH_3OH, mobile phase B was 0.05 M KH_2PO_4 (pH = 2.7), and the flow rates of mobile phase A and B were controlled to be 3% and 97%, respectively.[3] All mobile phases were vacuum-filtrated through a membrane filter (0.45 μm) before preparation and subsequently sonicated for 10 minutes to remove dissolved gases. The flow rate was 0.5 mL/min at a column oven temperature of 25 °C. The detection wavelength was 215 nm, and the injection volume was 20 μL. Before injection, phosphoric acid was used to adjust the pH of the sample to 2.7. In this method, the characteristic peak of formate appears around 7.2 minutes. The standard curve for formate is illustrated in Fig. S10.

The Faraday efficiency of gas and liquid products was calculated by the equation:

$$FE = \frac{Q_{product}}{Q_{total}} \times 100\% = \frac{nFv}{It} \times 100\%$$

Where $Q_{product}$ is the amount of electricity needed to produce the corresponding product (C), Q_{total} is the total charge passing through the working electrode (C), n is the number of electrons required for the corresponding product, F is the Faraday constant (96485 C/mol), v is the concentration of the corresponding product (mol), I and t represent the current (A) and time (S), respectively.

DFT Calculations

All density function theory (DFT) calculations were performed by the Vienna *Ab initio* Simulation Package (VASP), within the Projector Augmented Wave (PAW) method and the Perdew–Burke–Ernzerhof (PBE) functional for the exchange-correlation term being used.[4-6] The value of 400 eV was chosen for the kinetic energy cut-off of the electron wave functions. The convergence tolerances of the energy and forces were set to 1×10^{-4} eV and 0.05 eV/Å, respectively.[7, 8] The van der Waals interactions were considered by the DFT-D3 dispersion correction method.[9] The crystal surfaces of Cu (111) and CuCl (222) were used to construct the geometry structures. The free energy (G) was calculated using the equation:[10, 11]

$$G = E + ZPE - TS$$

Where E is the DFT-calculated energy changes of the optimized structures, ZPE is the zero-point energy correction and TS is the entropy correction at room temperature (T was set to be 300 K).

Values of ZPE and TS are respectively calculated by the equation:

$$ZPE = \frac{1}{2}\sum h\nu_i$$

$$TS = k_B T\left[\sum_i \ln\left(\frac{1}{1 - e^{-h\nu_i/k_B T}}\right) + \sum_i \frac{h\nu_i}{k_B T}\frac{1}{\left(e^{h\nu_i/k_B T} - 1\right)} + 1\right]$$

Where h is the Planck constant (6.62607015×10^{-34} J/s), v is the vibrational frequency (Hz), k_B is the Boltzmann constant (1.380649×10^{-23} J/K).

The following steps are considered for the CO_2 reduction to C_2H_4:[5]

1) $CO_2 + * \rightarrow *CO_2$
2) $*CO_2 + H^+ + e^- \rightarrow *COOH$
3) $*COOH + H^+ + e^- \rightarrow *CO + H_2O$

4) $*CO + CO \rightarrow *CO + *CO$
5) $*CO + *CO + H^+ + e^- \rightarrow *CO + *OCH$
6) $*CO + *OCH \rightarrow *OCCOH$
7) $*OCCOH + H^+ + e^- \rightarrow *OCC + H_2O$
8) $*OCC + H^+ + e^- \rightarrow *OCCH$
9) $*OCCH + H^+ + e^- \rightarrow *OHCCH$
10) $*OHCCH + H^+ + e^- \rightarrow *OH_2CCH$
11) $*OH_2CCH + H^+ + e^- \rightarrow *O + C_2H_4$
12) $*O + C_2H_4 + H^+ + e^- \rightarrow *OH + C_2H_4$

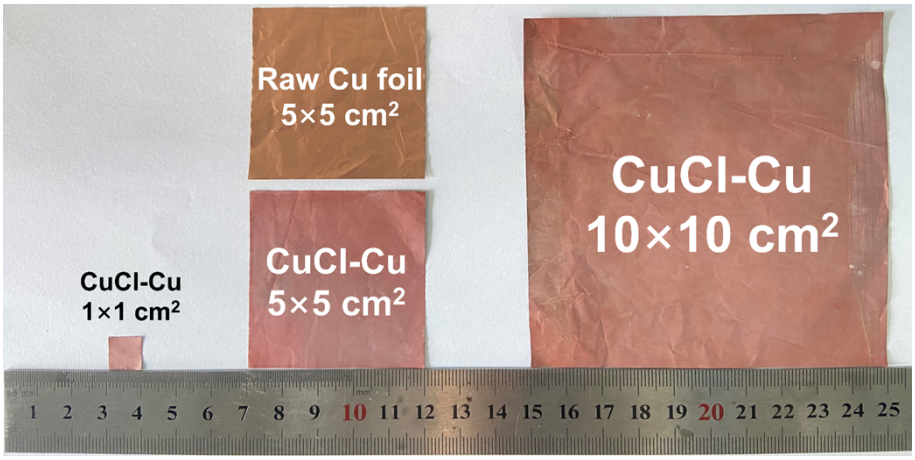

Fig. S1 Optical image of raw Cu foil and CuCl-Cu foil electrode in different sizes and a Raw Cu foil electrode.

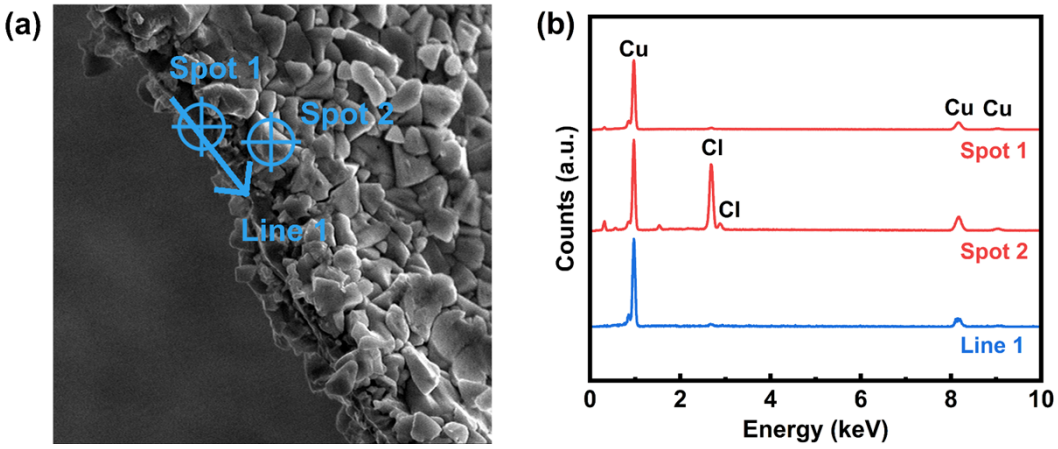

Fig. S2 (a) SEM images and (b) EDS analysis of the cross-section of CuCl-Cu electrode.

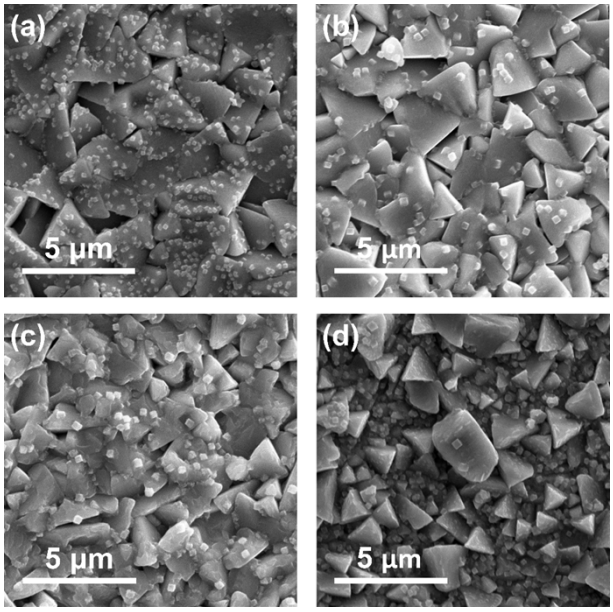

Fig. S3 CuCl-Cu prepared by different concentrations of $CuCl_2$ solution (a) 0.1 M, (b) 0.3 M, (c) 0.5 M, and (d) 0.7 M.

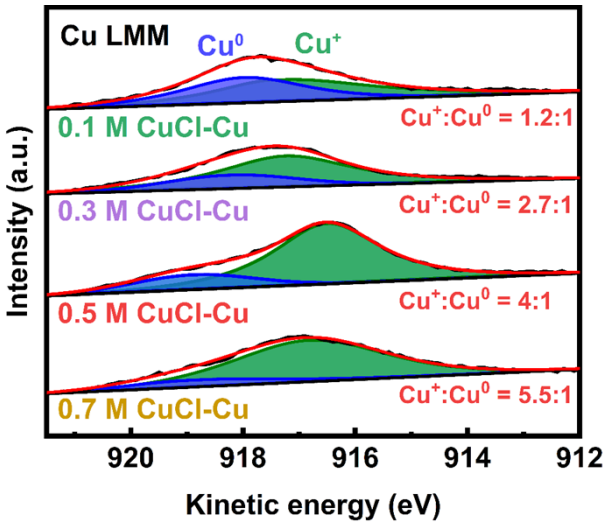

Fig. S4 high-resolution XPS of Cu LMM for 0.1 M CuCl-Cu, 0.3 M CuCl-Cu, 0.5 M CuCl-Cu, and 0.7 M CuCl-Cu.

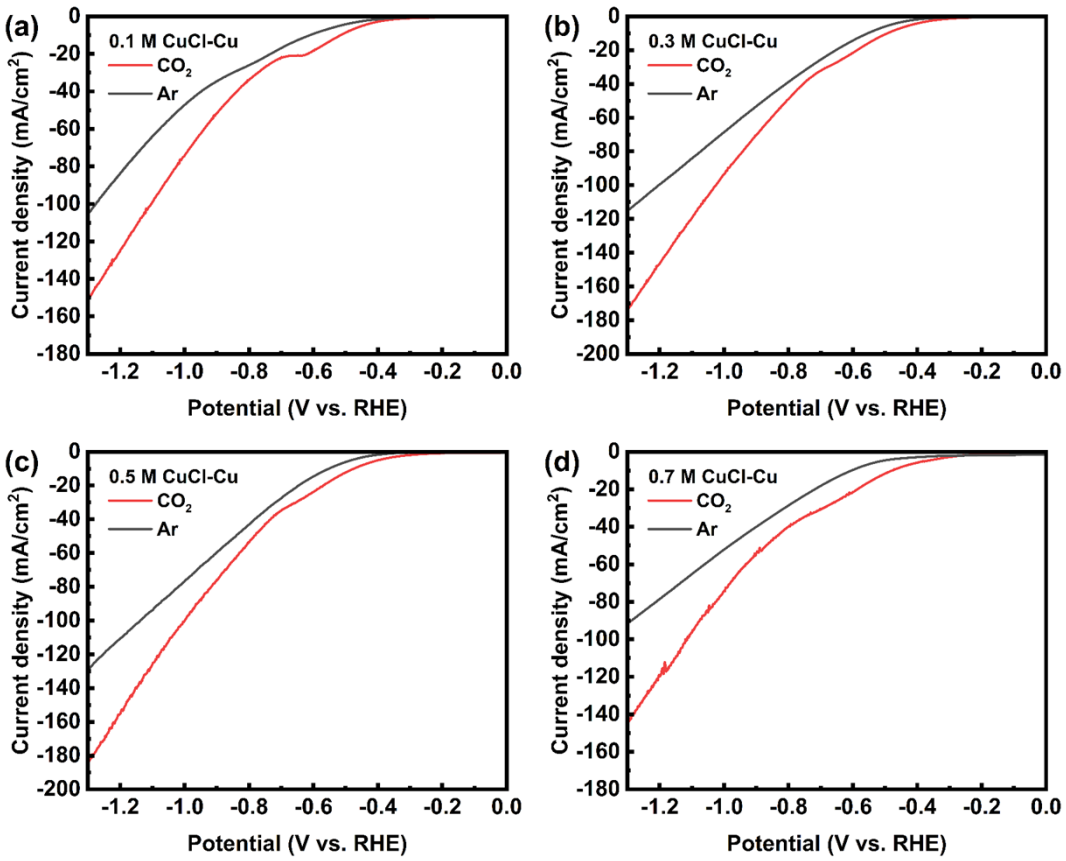

Fig. S5 LSV curves of CuCl-Cu in Ar or CO_2 atmosphere, (a) 0.1 M CuCl-Cu, (b) 0.3 M CuCl-Cu, (c) 0.5 M CuCl-Cu, and (d) 0.7 M CuCl-Cu.

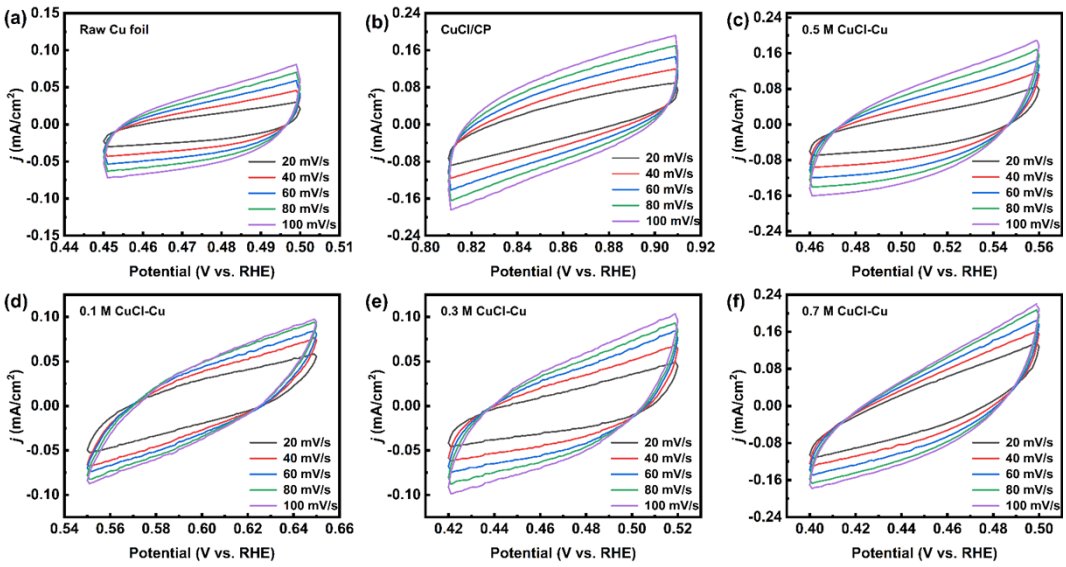

Fig. S6 Cyclic voltammetry curves of (a) Raw Cu foil, (b) CuCl/CP, (c) 0.5 M CuCl-Cu, (d) 0.1 M CuCl-Cu, (e) 0.3 M CuCl-Cu, and (f) 0.7 M CuCl-Cu scanned at the rate of 20, 40, 40, 60, 80, 100 mV/s.

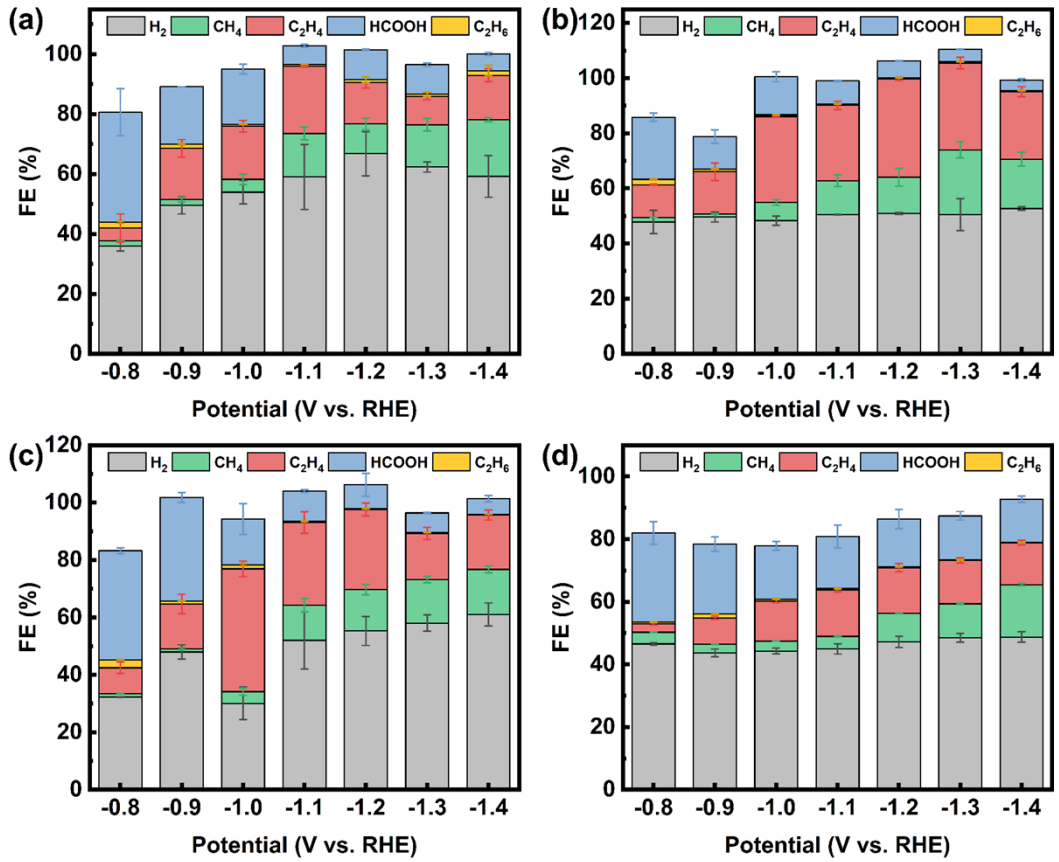

Fig. S7 The FEs of all products over (a) 0.1 M CuCl-Cu, (b) 0.3 M CuCl-Cu, (c) 0.5 M CuCl-Cu, and (d) 0.7 M CuCl-Cu at different applied potentials in 0.5 M $KHCO_3$.

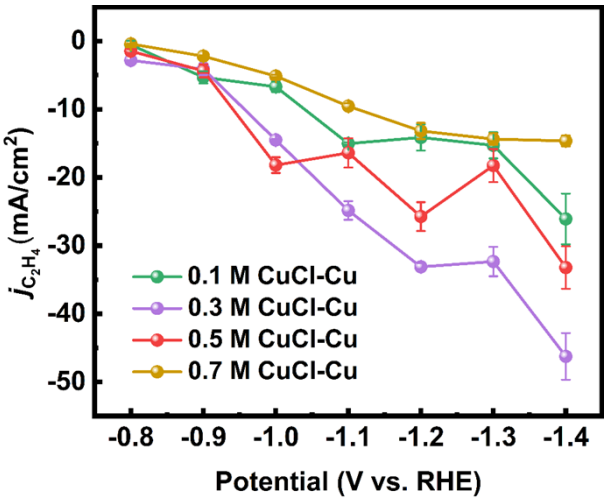

Fig. S8 Partial current density of C_2H_4 for different CuCl-Cu electrodes.

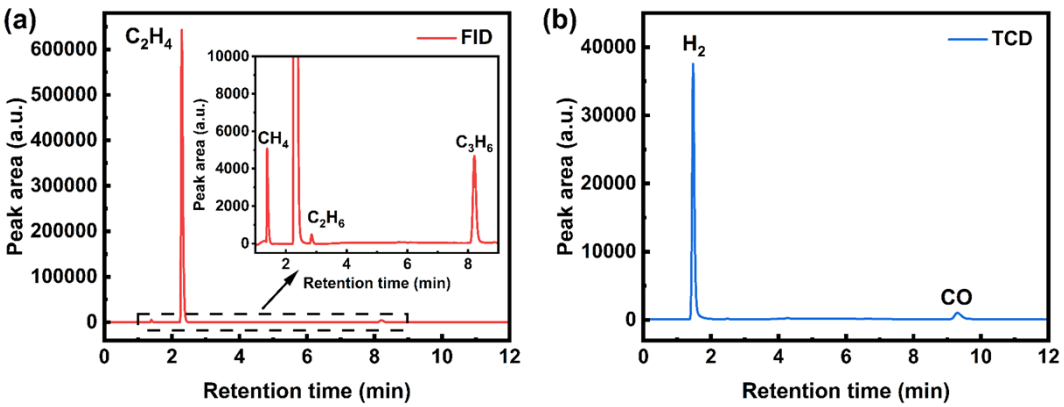

Fig. S9 GC spectra of the products for 0.5 M CuCl-Cu at −300 mA/cm^2, (a) FID, and (b) TCD.

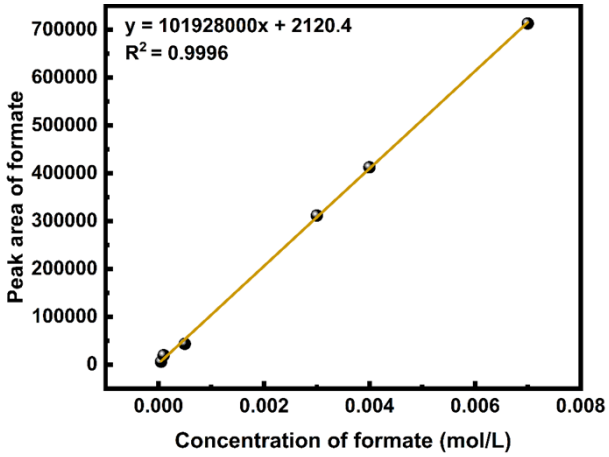

Fig. S10 Standard curve of formate for HPLC.

Catalyst	Electrolyte	Current density (mA cm^{-2})	$FE_{C_2H_4}$ (%)	References
De-Au_1Cu SAA	1 M KOH	–252	52	12
Cu-DEA-KB	2 M KCl	–308	50.5	13
50 wt% C_{60}/Cu(OH)F	0.1 M $KHCO_3$	-320	35	14
Cu_2O/CuO	1 M $KHCO_3$	-400	48.6	15
Cu_xO_y/CN	1 M KOH	-500	44	6
Cu-BIF/Cl	1 M KOH	-539	51.46	2
cAA-CuNW	1 M KOH	-888	60.7	7
0.5 M CuCl-Cu	**2 M KOH**	**-300**	**65.11**	**This work**

Table S1 CO_2-to-C_2H_4 conversion performance comparison of variously reported CO_2RR catalysts.

References

1 X. Yuan, S. Chen, D. Cheng, L. Li, W. Zhu, D. Zhong, Z. J. Zhao, J. Li, T. Wang and J. Gong, *Angew. Chem. Int. Ed.*, 2021, **60**, 15344-15347.
2 H. Guan, Y. Zhang, W. Fan, K. Yang, G. Li, S. Chen, L. Li and J. Duan, *Small*, 2024, **21**, 2406605.
3 S. Ma, K. Wu, S. Fan, P. Yang, L. Chen, J. Ma, L. Yang, H. Zhu and X. Ma, *Sep. Purif. Technol.*, 2024, **349**, 127926.
4 S. Zhong, H. Zhu, L. Yang, X. Chi, W. Tan and W. Weng, *J. Mater. Chem. A*, 2023, **11**, 8101-8109.
5 W. Liu, P. Zhai, A. Li, B. Wei, K. Si, Y. Wei, X. Wang, G. Zhu, Q. Chen, X. Gu, R. Zhang, W. Zhou and Y. Gong, *Nat. Commun.*, 2022, **13**, 1877.
6 N. Zhang and Y. Zhang, *J. Mater. Chem. A*, 2025, **13**, 2902-2910.
7 J. Kim, T. Lee, H. D. Jung, M. Kim, J. Eo, B. Kang, H. Jung, J. Park, D. Bae, Y. Lee, S. Park, W. Kim, S. Back, Y. Lee and D.-H. Nam, *Nat. Commun.*, 2024, **15**, 192.
8 J. Zhang, Y. Wang, Z. Li, S. Xia, R. Cai, L. Ma, T. Zhang, J. Ackley, S. Yang, Y. Wu and J. Wu, *Adv. Sci.*, 2022, **9**, 2200454.
9 T. Lv, J. Xiao, W. Weng and W. Xiao, *Adv. Energy Mater.*, 2020, **10**, 2002241.
10 J. Zhou, H. Xiao, W. Weng, D. Gu and W. Xiao, *J. Energy Chem.*, 2020, **50**, 280-285.
11 X. Zhou, J. Shan, L. Chen, B. Y. Xia, T. Ling, J. Duan, Y. Jiao, Y. Zheng and S.-Z. Qiao, *J. Am. Chem. Soc.*, 2022, **144**, 2079-2084.
12 Y. Zhao, Y. Wang, Z. Yu, C. Song, J. Wang, H. Huang, L. Meng, M. Liu and L. Liu, *ACS Nano*, 2025, **19**, 4505-4514.
13 Z. Lv, C. Wang, W. Liu, R. Liu, Y. Liu, X. Feng, W. Yang and B. Wang, *Adv. Energy Mater.*, 2024, **14**, 2402551.
14 X.-W. Xiong, X.-Y. Wu, Y.-S. Cheng, D. Yu, X.-D. Xu, Y.-W. Cheng, F.-H. Wu and X.-W. Wei, *Chem. Commun.*, 2025, **61**, 1681-1684.
15 H. Shi, L. Luo, C. Li, Y. Li, T. Zhang, Z. Liu, J. Cui, L. Gu, L. Zhang, Y. Hu, H. Li and C. Li, *Adv. Funct. Mater.*, 2023, **34**, 2310913.